First In Silico Simulation to Predict Inhibitors Targeting the HILPDA Protein in clear cell Renal Cell Carcinoma (ccRCC)

Rashmi Adulkar & Gaurav Sharma

Received December 08, 2025
Accepted May 18, 2025
Electronic access July 15, 2025

Kidney cancer remains a formidable global health challenge, claiming over 13,780 lives and affecting more than 76,000 individuals in the United States in 2021 alone. Among its subtypes, clear-cell renal-cell carcinoma (ccRCC) emerges as the most prevalent and aggressive form, characterized by aberrant formation of lipid droplets in cancerous cells. Recent research (2024) unveiled that the HILPDA protein helps produce lipid droplets by converting glutamine into fatty acids, fueling triglyceride accumulation and tumor progression. We hypothesize that small-molecule inhibitors bind to the predicted binding site of the HILPDA protein, thereby disrupting lipid metabolism and preventing the progression of ccRCC. To identify potential inhibitors, we screened 5,000 compounds and conducted molecular docking simulations using the AutoDock Vina software. Six ligands exhibiting strong binding affinities and favorable interaction profiles with HILPDA were selected. The docking simulations were validated by comparing them with the druggable sites on HILPDA predicted by P2Rank, a machine learning-based method (P2Rank). The SwissADME software evaluated ligands based on their interaction patterns, binding energies, and clinical viability metrics such as drug-likeness, blood-brain barrier permeability, and gastrointestinal absorption. All selected ligands demonstrated high gastrointestinal absorption, with several showing potential for blood-brain penetration. This research presents a novel therapeutic strategy for ccRCC, with the potential to reduce disease burden and significantly advance treatment approaches for one of the most lethal forms of kidney cancer.

Keywords: clear-cell renal-cell carcinoma (ccRCC), HILPDA, Computer Aided Drug Design, Molecular Docking, Machine Learning.

Introduction

About 70–80% of cases of kidney cancer are clear cell renal cell carcinoma (ccRCC), making it the most prevalent type of kidney cancer[1]. It starts in the proximal convoluted tubule's epithelial cells, an aspect of the kidney's filtering system[1]. Under a microscope, ccRCC is distinguished by its clear, pale cytoplasm[2]. Symptoms of the disease include blood in the urine, flank pain, and a palpable mass in the abdomen, although several cases are unintentionally discovered during imaging tests for unrelated illnesses[3]. The illness has the potential to spread quickly and aggressively, often spreading to distant organs like the liver, lungs, and bones[3]. Depending on the disease's stage and extent, treatment typically consists of immunotherapies, targeted therapies, and surgical resection[3]. Many patients nowadays have better outcomes due to the development of more effective targeted treatments based on a growing understanding of the genetic and molecular causes of ccRCC[3]. HILPDA plays a critical role in lipid metabolism and hypoxia signaling, both key hallmarks of clear cell renal cell carcinoma (ccRCC). Its overexpression in ccRCC tissues makes it a promising early detection biomarker and a potential therapeutic intervention target.

In this research, we have used molecular docking simulations, which use AutoDock Vina software. We can understand the binding pattern between a receptor and a ligand using this software. This method is prevalent in the drug discovery process as it can give a new chemical that can be used in the drug discovery process[4]. The software can be used to screen many

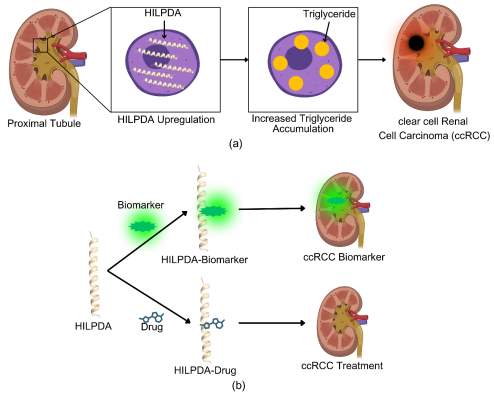

Fig. 1 clear cell renal cell carcinoma (ccRCC) formation in the kidney. (a) in ccRCC, the upregulation of HILPDA occurs, resulting in an increased triglyceride accumulation in cells; (b) HILPDA protein can be used as a ccRCC biomarker or targeted therapy.

chemical compounds and identify the one that binds strongly to the protein.

Lipid droplets (LD) are lipid-rich organelles that store lipids like triglycerides and cholesterol in cells[5]. Accumulation of LD is a common phenomenon in ccRCC[6]. These LDs function as energy storage and lipid metabolism dysregulation, and are linked to promoting cancer cell survival by providing energy to cancer cells. These ccRCC cells are characterized by a loss of von Hippel-Lindau (VHL) protein, which controls the hypoxia-inducible factor (HIF) pathway. Due to the loss of VHL protein, the activated HIF protein promotes the conversion of glutamine to fatty acids, resulting in lipid accumulation in cells. Recently, Sainero et al. have found that the HILPDA protein converts glutamine to fatty acids and causes an increased triglyceride accumulation in LDs[5]. Therefore, downregulation or inhibition of the HILPDA protein could be a potential therapeutic target for the disease. we hypothesize that small-molecule drugs can potentially bind and inhibit protein functioning. Therefore, we have performed a virtual screening of 5,000 ligands on the HILPDA protein and selected five ligands with a strong affinity for the protein. Later, the pharmaceutical properties of these ligands were also evaluated. This research work will help design novel inhibitors that can restrict the HILPDA protein and prevent lipid accumulation in LD.

Results

In the current study, we have worked on identifying inhibitors against the HILPDA protein, which disrupts lipid metabolism and leads to ccRCC. To identify potential ligands, we first characterized the structural features of the HILPDA protein and hypothesized that the ligands would preferentially bind to a predicted binding site on its surface. Hence, machine learning (ML) was used to find out whether it is possible to drug/ligand this specific spot. In particular, we used the P2Rank web server[7]. This is the druggable location in Figure 2a. The druggable location is indicated in red in this image. The electrostatic surface potential (ESP) of the receptor, as determined by the ChimeraX[8]. The distribution of electric charges on a protein's surface is measured by its electrostatic surface potential. It provides details on the interactions between the protein and other molecules.

After identifying the druggable site and evaluating its physicochemical properties, we investigated how potential ligands interact with this region through molecular docking simulations. To understand the HILPDA-ligand interaction, we performed molecular docking simulations using the HDOCK2.4 software[9]. we obtained the protein-ligand complexes after performing molecular docking simulations, as shown in Figure 2. The LigPlot software creates two-dimensional diagrams showing ligand-HILPDA interactions[10]. Due to these illustrations, it is simpler to comprehend how the ligand interacts with the protein's binding pocket or active site. LigPlot highlights hydrophobic interactions and hydrogen bonds between the ligand and the protein. The 2D image shows that the ligands formed hydrogen bonds and hydrophobic interaction with the HILPDA protein. The 3D image of the HILPDA-ligands complex was made using ChimeraX[8] software, which shows that all the ligands bind to a specific region, as shown in Figure 3.

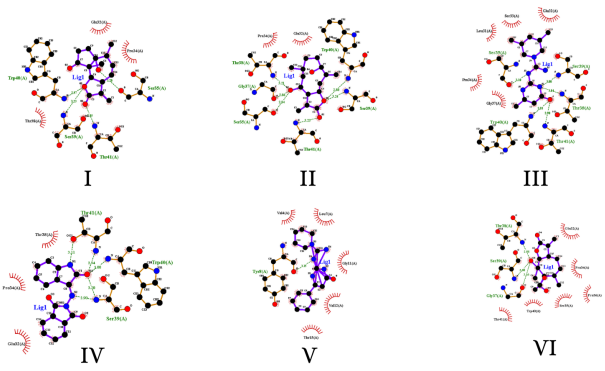

Fig. 2 2D image of ligands and amino acids. This figure shows that the amino acids (orange) bind to the ligand (purple) by hydrophobic and hydrogen bonds.

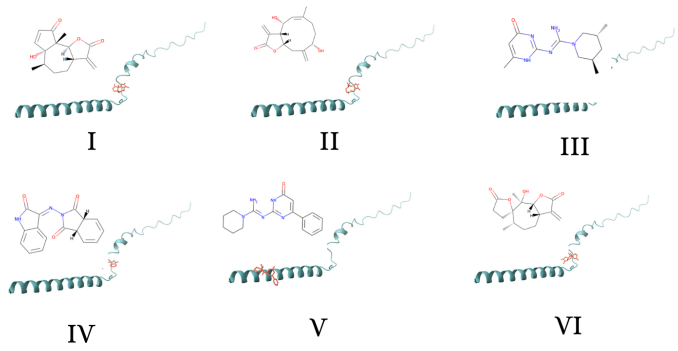

Fig. 3 3D structure. All the ligands (except Ligand V) bind to the same site.

To further characterize these interactions and validate the docking results, we analyzed the specific bonding patterns between the ligands and the HILPDA protein. The following analysis was the interaction formed between the HILPDA-ligands complexes. This was done using the PLIP software[11]. Based on this, we formed one hydrophobic interaction and five hydrogen bonds. In addition, ligand II formed one hydrophobic interac-

tion and six hydrogen bonds. Moreover, ligand III formed two hydrophobic interactions and seven hydrogen bonds. Similarly, Ligand IV formed three hydrophobic interactions and six hydrogen bonds. Next, Ligand V formed six hydrophobic interactions and two hydrogen bonds. Lastly, Ligand VI formed one hydrophobic interaction and four hydrogen bonds. Finally, we have also predicted the binding energy of the HILPDA-ligands complex, as shown in Table 2. According to binding energy, all ligands form binding energy similar to that of the HILPDA protein.

Beyond analyzing molecular interactions, we further evaluated the pharmacokinetic properties of the selected ligands to assess their potential as drug candidates. The pharmaceutical properties of the selected ligands were predicted, and three properties were computed. Gastrointestinal absorption: The process by which nutrients and other substances are absorbed into the bloodstream from the digestive tract is known as intestinal absorption. Blood-brain barrier permeation: Permeation of the blood-brain barrier is the process by which substances cross the selective barrier that lets necessary molecules in but shields the brain from potentially dangerous substances; and (c) drug likeliness: The degree to which a material satisfies the requirements for drug development, such as sufficient absorption, distribution, digestion, and excretion, is referred to as drug likeliness. Based on this, all the ligands have high GI absorption. High gastrointestinal (GI) absorption is desirable because the drug can be effectively administered orally and easily absorbed in the digestive tract. The drug should also be highly water-soluble for optimal oral administration, facilitating its dissolution and absorption in the stomach. Improved GI absorption enhances the drug delivery process and increases bioavailability, making the treatment more effective. However, ligands I and II were BBB permeant, and Ligands III, IV, V, and VI were not. All the ligands show high drug-likeliness. Finally, we have also computed the binding energy between the protein-ligand complex, and all the ligands show similar binding energy. Figure 4 shows the number of interactions formed between the protein and the ligands, highlighting both hydrophobic interactions and hydrogen bonds. Based on these interactions, most ligands form a higher number of hydrogen bonds. Since hydrogen bonds are generally stronger than hydrophobic interactions, we assume that Ligand 3 is the strongest binder to the protein

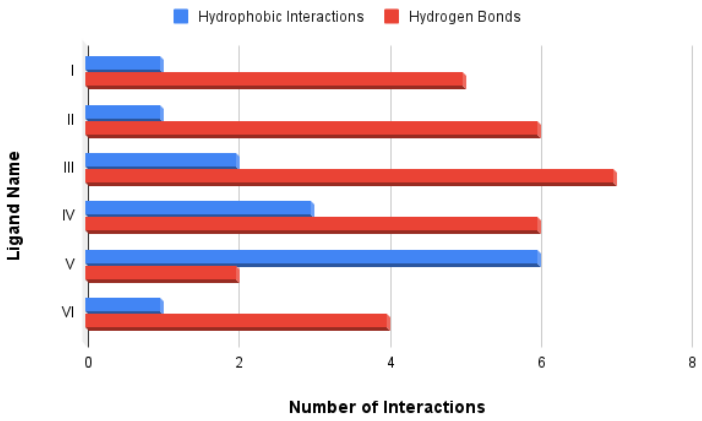

Fig. 4 Interactions bar graph. The bar graph shows the number of interactions formed between the HILPDA-Ligand complexes.

Discussion

The protein known as VHL, or Von Hippel-Lindau, degrades the HIFα and HIFβ proteins[12]. Degrading HIFα and HIFβ prevents them from accumulating in the renal cell. HIFα and HIFβ control how cells respond to low oxygen levels, helping them to survive and function better at low oxygen levels[13]. In the absence or with the malfunction of VHL, HIFα, and HIFβ get overactivated[14]. The overactivation causes the conversion of glutamine to lipids/fatty acids inside renal cells and results in its accumulation inside cells[14]. The overabundance of lipids accumulating in renal cells causes the growth and progression of ccRCC[14]. clear cell renal cell carcinoma (ccRCC) is characterized by altered lipid metabolism, including the accumulation of lipid droplets and increased fatty acid synthesis, which supports tumor growth and survival. Several inhibitors targeting these lipid metabolic pathways have shown potential in ccRCC therapy. Fatty acid synthase (FASN) inhibitors such as TVB-2640 (Denifanstat), currently in phase II clinical trials for various cancers, block de novo lipogenesis and have shown promise in inhibiting ccRCC progression. Additionally, stearoyl-CoA desaturase 1 (SCD1) inhibitors like A939572 and CAY10566 disrupt the production of monounsaturated fatty acids, leading to impaired lipid homeostasis and reduced tumor viability. These agents are being investigated in preclinical and early-phase clinical studies. Another notable target is ATP-citrate lyase (ACLY), a key enzyme linking glucose metabolism to lipid synthesis, and its inhibition has demonstrated anticancer effects in ccRCC models. Moreover, inhibition of the HILPDA protein, which promotes lipid droplet formation in ccRCC cells, is an emerging strategy explored through molecular docking and in silico screening. Overall, targeting lipid metabolism represents a promising therapeutic approach for ccRCC. However, most of these inhibitors are still under investigation and not yet approved for clinical use in this cancer type.

The formation of lipid droplets in renal cells, which results in an excessive build-up of fatty acids, is associated with the HILPDA protein[5]. clear cell renal cell carcinoma (ccRCC) is linked to the incidence and development of this accumulation[5]. One effective way to interfere with lipid metabolism and slow down the progression of the disease is to target HILPDA. Small molecules should target specific binding sites on HILPDA to inhibit its function and possibly cause disruptions to lipid accu-

mulation in ccRCC cells. Our molecular docking simulations used various chemical compounds to find possible inhibitors. This strategy aimed to identify the substances that could bind to the HILPDA protein and block its function. Based on our simulations, six ligands with binds to the HILPDA protein were found.

After performing molecular docking simulations and virtual screening and identifying a few promising ligands (such as four or five), it is essential to validate their binding affinity and inhibitory potential through computational and experimental techniques. Initially, post-docking validation methods such as molecular dynamics (MD) simulations can be used to assess the stability of the ligand-protein complex over time, followed by free energy calculations like MM/PBSA or MM/GBSA to estimate binding energies more accurately. Subsequently, experimental validation techniques should be employed. Surface Plasmon Resonance (SPR) and Isothermal Titration Calorimetry (ITC) can provide real-time binding affinity measurements and thermodynamic parameters. Additionally, enzyme inhibition assays or cell-based assays can be conducted to confirm whether the ligands effectively inhibit the biological activity of the target protein. Other techniques, such as X-ray crystallography or NMR spectroscopy, can be used to determine the structural conformation of the ligand-bound protein complex. These steps collectively ensure the reliability of the in-silico predictions and help transition from computational modeling to potential therapeutic development.

Some of the limitations of this research are as follows: Since our study was computational, in future work, we will try to include lab experiments to validate the computational results. Moreover, in ccRCC, the lipid accumulates inside the cells and could decrease the drug penetration inside the cancer cells. Since the HILPDA protein is present inside the cell, it would be difficult for the drug to bind to the protein. One of the potential strategies to overcome this hurdle is to modify the ligands to make them more lipid-soluble chemically. Moreover, lipid-based nanoparticles carrying the drug could surpass this barrier and help deliver the drug to the cancer cell.

In conclusion, this research effectively identifies the HILPDA protein as a possible target for treatment in cases of clear cell renal cell carcinoma (ccRCC). Using virtual screening of 5000 ligands and molecular docking, six molecules forming strong interactions with HILPDA protein were identified. Significant hydrophobic contacts and hydrogen bonding between these ligands and the protein suggest that they may effectively block HILPDA and, as a result, lower the buildup of triglycerides in lipid droplets. Furthermore, predictions derived from machine learning verified that the binding location on HILPDA is druggable. This work offers a potential for developing new inhibitors that target the disruption of lipid metabolism to improve the treatment of ccRCC.

Method

The HILPDA protein amino acid sequence was obtained from the UniProt website, and the amino acids were uploaded on the AlphaFold 3 server[15]. Ligands were downloaded from the Zinc20 database in the PDBQT format[16]. Molecular docking was performed using AutoDock Vina software to obtain the HILPDA-ligand complexes[17]. Docking is a technique used in molecular modeling that predicts a molecule's preferred orientation to a second when a ligand and a target are joined to create a stable complex. HILPDA protein and ligand interactions were obtained using the PLIP software[11]. The HILPDA-ligand complexes 2D structures were made using the LigPLOT software[10]. The HILPDA-ligand complexes 3D structures were made using the ChimeraX software[8]. The three-dimensional arrangement of atoms in a molecule is called molecular geometry or molecular structure.

References

1 D. J. Grignon and M. Che, *Critical Issues in Laboratory Medicine*, 2005, **25**, 305–316.

2 R. A. Gibbs, D. A. Wheeler *et al.*, *Nature*, 2013, **499**, 43–49.

3 R. E. Gray and G. T. Harris, *American Family Physician*, 2019, **99**, 179–184.

4 J. Fan, A. Fu and L. Zhang, *Quantitative Biology*, 2019, **7**, 83–89.

5 L. Sainero-Alcolado, E. Garde-Lapido, M. T. Snaebjörnsson, S. Schoch, I. Stevens, M. V. Ruiz-Pérez and A. Schulze, *Proceedings of the National Academy of Sciences*, 2024, **121**, e2310479121.

6 G. Xu, Y. Jiang, Y. Xiao, X.-D. Liu, F. Yue, W. Li and H. Huang, *Oncotarget*, 2016, **7**, 6255.

7 R. Krivák and D. Hoksza, *Journal of Cheminformatics*, 2018, **10**, 1–12.

8 E. F. Pettersen, T. D. Goddard, C. C. Huang, G. S. Couch, D. M. Greenblatt, E. C. Meng and T. E. Ferrin, *Journal of Computational Chemistry*, 2004, **25**, 1605–1612.

9 Y. Yan, H. Tao, J. He and S.-Y. Huang, *Nature Protocols*, 2020, **15**, 1829–1852.

10 A. C. Wallace, R. A. Laskowski and J. M. Thornton, *Protein Engineering, Design Selection*, 1995, **8**, 127–134.

11 S. Salentin, S. Schreiber, V. J. Haupt, M. F. Adasme and M. Schroeder, *Nucleic Acids Research*, 2015, **43**, W443–W447.

12 J. An and M. B. Rettig, *Journal of Molecular Biology and Cancer*, 2005.

13 A. Bouthelier and J. Aragonés, *Biochimica et Biophysica Acta - Molecular Cell Research*, 2020, **1867**, 118733.

14 M. Miro-Murillo, A. Elorza, I. Soro-Arnaiz, L. Albacete-Albacete, A. Ordonez, E. Balsa and C. Fernandez-Criado, *PLOS ONE*, 2011, **6**, e22589.

15 J. Abramson, J. Adler, J. Dunger, R. Evans, T. Green, A. Pritzel and J. J. N. Bambrick, *Nature*, 2024, 1–3.

16 J. J. Irwin, K. G. Tang, J. Young, C. Dandarchuluun, B. R. Wong, M. Khurelbaatar *et al.*, *Journal of Chemical Information and Modeling*, 2020, **60**, 6065–6073.

17 G. M. Morris, D. S. Goodsell, R. Huey, W. E. Hart, S. Halliday, R. Belew and A. J. Olson, *Automated Docking of Flexible Ligands to Receptors Using Genetic Algorithms*, 2001.

Table 1 HILPDA-ligand interactions. The table shows the bonds formed in docking simulations.

I		
Hydrophobic Interactions	**Amino acids**	**Distance (Å)**
	Pro34	3.51
Hydrogen Bonds	Thr38	3.31
	Ser39	2.24
	Trp40	2.17
	Thr41	2.11
	Thr41	2.43
II		
Hydrophobic Interactions	**Amino Acids**	**Distance (Å)**
	Pro40	3.66
Hydrogen Bonds	6	2.4
	Thr38	2.47
	Ser39	2.84
	Trp40	2.94
	Thr41	2.43
	Thr41	2.48
III		
Hydrophobic Interactions	**Amino Acids**	**Distance (Å)**
	Glu32	3.77
	Pro34	3.72
Hydrogen Bonds	Ser35	2.23
	Thr38	2.93
	Ser39	3.35
	Ser39	2.25
	Trp40	2.06
	Thr41	2.1
	Thr41	2.35
IV		
Hydrophobic Interactions	**Amino Acids**	**Distance (Å)**
	Glu32	3.78
	Glu32	3.52
	Pro24	3.77
Hydrogen Bonds	Thr38	3.35
	Ser39	2.2
	Trp40	2.03
	Thr41	2.14
	Thr41	2.4
	Thr41	2.46
V		
Hydrophobic Interactions	**Amino Acids**	**Distance (Å)**
	Leu7	3.81
	Tyr8	4
	Tyr8	3.59
	Tyr8	3.88
	Val12	3.48
	Thr15	3.98
Hydrogen Bonds	Tyr8	2.38
	Gyl11	3.57
VI		
Hydrophobic Interactions	**Amino Acids**	**Distance (Å)**
	Glu32	3.94
Hydrogen Bonds	Ser35	3.08
	Thr38	1.93
	Ser39	2.62
	Ser39	3.29

Table 2 Pharmaceutical properties of selected ligands. The table shows that all the ligands have high GI absorption, and Ligands I and II also have high BBB absorption. Finally, the binding energy between HILPDA-ligand is displayed in the last row.

	I	**II**	**III**	**IV**	**V**	**VI**
Formula, molecular weight	C15H18O4O, 262.30 g/mol	C15H20O4, 264.32 g/mol	C13H21N5O, 263.34 g/mol	C16H11N3O3, 293.28 g/mol	C16H19N5O, 297.35 g/mol	C15H20O5, 280.32 g/mol
Gastrointestinal Absorption	High	High	High	High	High	High
Blood Blood-brain barrier permeation	Yes	Yes	No	No	No	No
Drug likeliness (Lipinski)	Yes	Yes	Yes	Yes	Yes	Yes
Binding Energy (kcal/mol)	-5.29	-5.28	-5.2	-5.13	-5.26	-5.28